RSC Sustainability

ROYAL SOCIETY OF CHEMISTRY

PAPER

View Article Online
View Journal | View Issue

Cite this: *RSC Sustainability*, 2026, 4, 1933

Cracking behavior of upgraded waste plastic pyrolysis oil to lighter olefins (C_2–C_3): a study on performance, product distribution and outlook for a circular hydrocarbon economy

Abhishek G. Sarang,†[a] Aditya Bora,†[a] Syed Mohammed Razak,[ab] Karan Sharma,[a] Chandan Kumar Munagala,[ab] Pratik Mali,[a] Nettem V. Choudary[b] and Vineet Aniya *[ab]

Circularity in plastic waste management is still a major challenge due to the heterogeneous nature of plastic waste streams, which find use in generators but face restrictions in wider applications. Chemical upgradation of plastic pyrolysis oil offers a practical route to improve fuel compatibility and usability. The proposed treatment approach shows flexibility across different feedstock conditions, supporting its relevance for closed-loop plastic recycling. This study investigates the catalytic cracking of upgraded waste plastic pyrolysis oils (PPO), including chemically treated (CPO) and distilled (DPO) pyrolysis oils. Cracking was done using Equilibrium Catalyst (E-CAT) in a fixed-bed reactor, operating within the temperature range of 500 °C to 600 °C to produce light olefins (C_2–C_3). The influence of DPO, CPO, and PPO on product distribution and catalyst performance is examined. The findings reveal that DPO yields the highest cracking toward light olefins, with a yield of 61.1 mol% at 550 °C and a WHSV of 2 h^{-1} as compared to CPO and PPO. In contrast, CPO and DPO resulted in higher conversions of methane (26.4 mol% and 25.7 mol%, respectively), followed by the lowest in DPO (17 mol%). Time-on-stream analysis (TOS) revealed that DPO's lighter olefin conversion has declined, particularly in ethylene yield from 31.09 mol% to 12.13 mol% over time as compared to CPO, which maintained an ethylene yield of 23.5 mol%. This study contributes to the prospect of upgraded PPO as an alternative to naphtha feed under optimized reaction conditions, such as temperature and WHSV, for high yields of olefins in a petrochemical unit.

Received 21st December 2025
Accepted 12th February 2026

DOI: 10.1039/d5su00937e

rsc.li/rscsus

Sustainability spotlight

The present highlights the sustainable valorisation of plastic waste by converting upgraded waste plastic pyrolysis oils (PPO) into light olefins, essential building blocks for the petrochemical industry. By employing catalytic cracking with a spent FCC catalyst, the process not only offers a circular pathway for managing plastic waste but also reduces reliance on fossil-based naphtha feedstocks. Optimizing reaction conditions for higher olefin yields demonstrates a dual benefit addressing the global plastic waste challenge while enabling resource-efficient, low-carbon feed alternatives for petrochemical production.

1 Introduction

The future of the petrochemical sector in India is bright, as the industry is anticipated to draw investments exceeding US$87 billion over the next decade, with the country accounting for more than 10% of global petrochemical growth. Light olefins such as ethylene and propylene play a central role in this growth, with ethylene alone acting as the raw material for 75% of petrochemical products, including polyethylene (PE), ethylene oxide, ethylene dichloride, *etc.* Propylene is another key feedstock for the production of essential commodities such as polypropylene (PP), propylene oxide, acrylonitrile, *etc.*, and this key raw material is expected to experience steady growth, with its demand projected to maintain a CAGR of 4.26% over the next 10 years.[1] India's polymer demand is likely to outperform domestic capacity addition over the next decade. While primary petrochemical capacity is increasing at a CAGR of approximately 6%, net imports of fossil-based feedstocks have risen at a CAGR of 19%.[2] At present, light olefins (C_2–C_3) are primarily manufactured by subjecting fossil-derived naphtha to

[a]*Process and Polymer Engineering Lab, Chemical Engineering and Process Technology Department, CSIR-Indian Institute of Chemical Technology, Hyderabad, 500007, India. E-mail: vineetkumaraniya@gmail.com; vineet@csiriict.in; Fax: +9140-2711234; Tel: +9140-27191396*

[b]*Academy of Scientific and Innovative Research (AcSIR), Ghaziabad, 201002, India*

† These authors contributed equally to the present study.

steam cracking.[3] India's heavy reliance on fuel imports poses economic risks due to volatile oil prices.[4] To minimize these risks, it is necessary to explore other potential sources that can be retrofitted into the existing systems to derive light olefins. In this context, end-of-life plastics are gaining attention as a practical and increasingly viable option.[5]

Presently, the extensive use of plastics due to their versatile applications in daily human life has led to a well-known global plastic crisis.[6] The manufacturing and disposal of plastic products drastically raise pollution of the air, land, and water.[7] Consequently, the proliferation of plastic waste poses severe threats to ecosystems, marine life, and human health, necessitating urgent and effective waste management and recycling solutions.[8] To address these issues, there is significant interest in tertiary recycling through thermochemical processes; one such process is pyrolysis.[9] The primary product of plastic pyrolysis is the pyrolytic oil comprising C_5–C_{40} hydrocarbons.[10] The pyrolysis technology for plastic waste has been extensively researched and has had successful commercialization over the past two decades.[11,12] However, commercially available plastic pyrolysis oil presents several challenges. The oil derived from waste plastic contains large amounts of particulate matter, heavy elements, heavy hydrocarbons, and sulfur, as well as exhibiting higher viscosity than conventional fuels.[13,14] These issues limit the applications of waste plastic pyrolysis oils to low-end use cases such as furnace oils and boiler fuels.[15–17] This plastic oil has the potential to be recycled into fundamental building blocks such as C_2–C_3, thereby enabling closed-loop recycling.[18,19]

More recent investigations continue to explore new catalytic systems and reaction conditions to optimize the selectivity and yield of light olefins. Raghav *et al.* (2025), for example, explored the *in situ* catalytic pyrolysis of LDPE over a manganese-supported alumina catalyst, reporting a light olefin yield of 47.9% in the gaseous products at 400 °C.[20] Diao *et al.* (2025) developed a tandem catalytic cracking system using an interconnected Al–SiO_2 catalyst and achieved an impressive light olefin yield of 50 wt%.[21] Further modification of current approaches is necessary to eliminate catalyst poisons effectively and increase process efficiency.[22] Increasing yields of light olefins while lowering challenges like corrosion and catalyst deactivation requires improvements in chemical treatment, distillation, and reaction conditions. Several studies have investigated using zeolites to convert olefins, using model plastic oil, into aromatics and short-chain olefins,[23–25] but by using waste plastic pyrolysis oil, Tran *et al.* (2024) obtained a 56.6% yield of light olefins.[26] Although the pyrolysis industry is experiencing rapid growth with plastic oils finding applications in industrial furnaces, this approach provides a pathway for refineries to function in olefin production. While several studies have explored the catalytic conversion of model hydrocarbons or partially purified pyrolysis oils, limited work has systematically compared crude, chemically treated, and distilled waste plastic pyrolysis oils under identical catalytic cracking conditions for lighter olefin production to understand their true industrial viability. This approach increases the economic potential of plastic waste by developing a cost-effective process for light olefin production using E-CAT. The study aims to prioritize creating a circular economy solution by identifying the most suitable upgraded oil and optimal operating parameters that not only address plastic waste management but also reduce dependence on fossil-based naphtha, with sustainability and industrial feasibility as key priorities for seamless integration into existing petrochemical infrastructure.

2 Materials and methods

2.1 Materials

The crude waste plastic pyrolysis oil (PPO) used in the current study was procured from 2 Degrees Clicon, Hyderabad. PPO was produced *via* batch catalytic pyrolysis of mixed polyolefin waste comprising LDPE, HDPE, and PP at 450 °C. The spent commercial FCC catalyst (E-Cat) was provided by Mangalore Refinery and Petrochemical Ltd, India. Chemicals such as sulfuric acid (98%), formic acid, and hydrogen peroxide (30% w v^{-1}) were procured from Finar Pvt Ltd, India. Polyvinyl alcohol (PVA) was procured from Loba Chemie Pvt Ltd, and calcium oxide was sourced from Avra Laboratories Pvt Ltd.

2.2 Oil upgradation

2.2.1 Chemically upgraded pyrolysis oil (CPO). 1000 g of waste plastic pyrolysis oil (PPO) was first treated with 8% w/w sulfuric acid at 50 °C for 240 min and later centrifuged for 15 min at 4000 rpm, resulting in the formation of two separate layers. The upper layer underwent additional processing, while the lower layer, composed of thick acidic sludge, was disposed of. To prevent wax formation during storage, this oil was then treated with a mixture containing 5% w v^{-1} calcium oxide, agitated with a magnetic stirrer, and kept at 70 °C for 240 min. To extract the oil from the spent powder adsorbents, the mixture went through centrifugation. 780 g (with a mass loss of 22 wt% of PPO) of oil is collected as CPO and used for further studies. This loss is attributed to the removal of acidic sludge, suspended carbonaceous matter, and metal impurities.

2.2.2 Distilled pyrolysis oil (DPO). Furthermore, 780 g of CPO is subjected to distillation by heating to 350 °C at a ramp rate of 1 °C min^{-1}. The resulting distilled fraction then undergoes an oxidative desulfurization step. Herein, a mixture of 100 g, consisting of 10 g of 98% formic acid, 20 g of 30% hydrogen peroxide, and the remaining water, was prepared and used to treat the distilled fraction of CPO. After stirring at 350 rpm and heating the mixture for 120 min at 60 °C, it was allowed to rest overnight. Upon being separated, the upper layer of clear pyrolysis oil was cleaned with 20% v/v distilled water. To eliminate all molecular moisture, the oil was lastly filtered through a bed of anhydrous sodium sulfate to obtain distilled pyrolysis oil (DPO). Overall, the DPO yield was 540 g (with a mass loss of 31 wt% of CPO).

2.3 Catalyst preparation

To prepare catalyst pellets using a binder-assisted method, 6 g of polyvinyl alcohol (PVA) was dissolved in 30 ml of deionized water while being continuously stirred at 700 rpm for 30 min. In

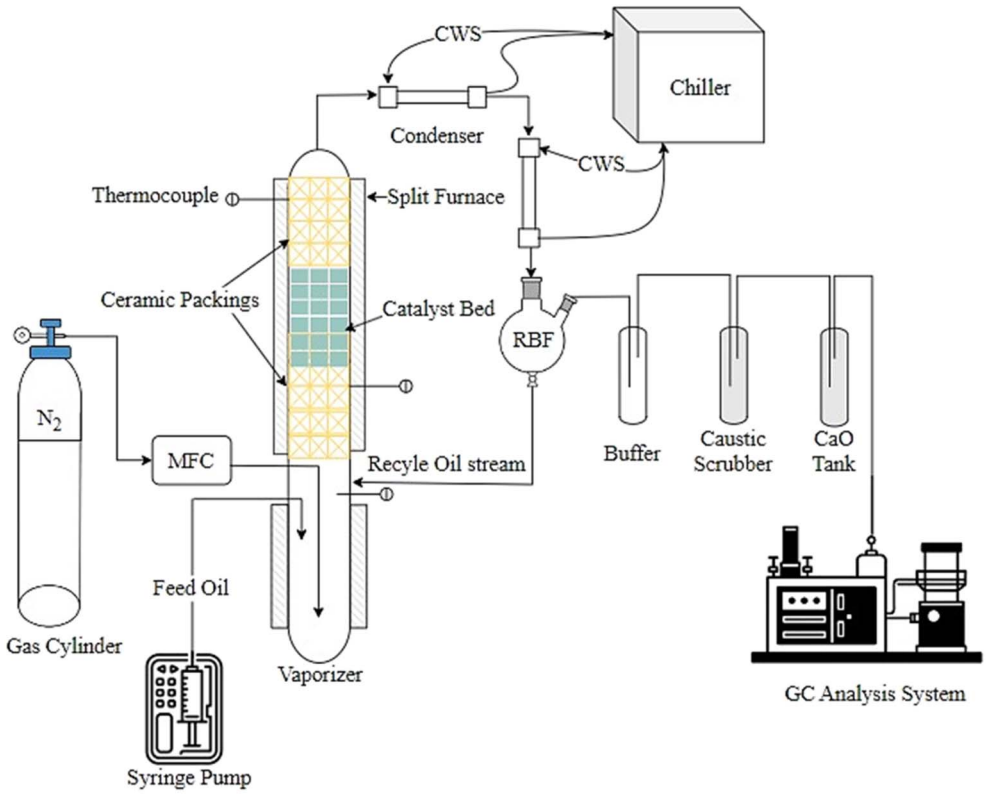

Fig. 1 Schematic of the experimental setup.

order to ensure that the binder was evenly distributed throughout the catalyst matrix, 100 g of spent commercial FCC catalyst powder was gradually added under stirring until a homogeneous mixture was obtained. The resulting slurry was then placed in a tray and dried overnight at 120 °C in a drying oven. The solidified mixture was crushed using a 2 mm sieve plate after drying. The processed material was then pelletized into cylindrical pellets, measuring 4 mm in diameter and height, for catalytic applications. The prepared catalyst was calcined at 600 °C for 180 min and used for oil cracking.

2.4 Olefin recovery experiments

The prepared FCC catalyst was packed in a quartz column of 700 mm in length with a volume of 350 ml, with 80% of the reactor volume filled with inert packing. This column was placed in a 500 mm-long split furnace. The portion of the reactor extending outside the furnace was well insulated. The reaction time was 1 h, and the fixed bed temperature was varied between 500 °C and 600 °C, at atmospheric pressure. The oil was fed using a syringe pump at a WHSV between 0.2 h^{-1} and 2 h^{-1} into a vaporiser maintained at 370 °C, which was attached to the bottom of the catalytic column. The quenching of gas was achieved by coupling two condensers in series, such that the second condenser was attached to a two-necked RBF while the first condenser was directly connected to the catalytic column. The cold-water supply for the condensers was provided by chillers maintained at 4 °C. Condensed vapors were recycled in the vaporizer, and the non-condensable gases passed through the buffer tank and treated in a two-stage system, first neutralizing toxic materials in a caustic tank, followed by moisture removal in a calcium oxide tank. Two-stage condensation was used to avoid any carry-over of condensable species into the gas trap. To avoid unwanted gas interactions, a continuous nitrogen flow at 5 ml min^{-1} was used to purge the system before starting the reactions, as shown in Fig. 1. The experiments initially utilized distilled pyrolysis oil (DPO), and the optimal conditions were applied to PPO and CPO. The ethylene and propylene production over time was studied over a 24 h period for upgraded oils.

2.5 Materials characterization

2.5.1 Oil characterization. The density of each oil type was measured using a densitometer, and the viscosity was determined using a Borosil Man Singh Survismeter. A Vario Micro Cube Elemental Analyzer was utilized to perform the ultimate analysis. A Thermo Scientific iCAP 7200 model with a CETAC AXP 560 autosampler (Teledyne Technology, USA) and Qtegra Software (Thermo Scientific iCAP 7000 Plus Series ICP-OES, Thermo Fisher Scientific Brand, USA) was used to conduct metal analysis. Detailed physicochemical parameters were investigated using ASTM procedures.[27] A GC-MS unit (Agilent 6890 with a 5973N detector) fitted with an HP-5MS capillary column (30 m, 250 μm ID, 0.25 μm film) was used to examine the oil composition. Helium served as the carrier gas, and the oven temperature was ramped from 50 °C to 280 °C at a rate of 10 °C min^{-1}. The range of mass spectrometry was 29 m z^{-1} to

600 m z^{-1}. The fragments were identified using the Wiley Registry and NIST databases.

2.5.2 Gas analysis. The gas samples collected for compositional analysis of Waste Plastic Pyrolysis Oil (PPO), Distilled Pyrolysis Oil (DPO), and Chemically Treated Pyrolysis Oil (CPO) were analyzed using Gas Chromatography equipped with a FID and a VF-1ms capillary column (15 m × 0.25 mm × 0.25 μm). The injection temperature was set at 280 °C, with a column flow rate of 1 ml min^{-1}. Hydrogen, nitrogen, and air were supplied at 30, 25, and 300 ml min^{-1}, respectively. The run started at 50 °C with a 1 min hold, then the temperature was raised at 8 °C min^{-1} to 150 °C without a hold, followed by a 10 °C min^{-1} increase to 280 °C, where it was held for 0.50 min.

2.5.3 Catalyst characterization. The Oxford INCA 400 EDX unit was paired with a Carl Zeiss Supra 55VP system to examine the chemical composition and perform FESEM imaging of the catalyst surface. A Micromeritics ASAP 2010 analyzer was used to obtain surface-area data through the BET method. At −196 °C, N_2 physisorption isotherms were measured to evaluate the catalyst's surface area and porosity. FTIR analysis was carried out on the crushed catalyst mixed with KBr and sieved to obtain particles smaller than 75 μm. 64 scans were recorded across a 400–4000 cm^{-1} region. Catalyst acidity was assessed through NH_3-TPD measurements. The sample was pretreated under helium flow to remove adsorbed impurities, saturated with NH_3 at 100 °C, and then purged to remove physiosorbed NH_3. Desorption was carried out by linear heating to 900 °C, and the desorbed NH_3 was quantified using a TCD.

3 Results and discussion

3.1 Oil characterization

The compositional analysis of Plastic Pyrolysis Oil (PPO), Chemically treated Pyrolysis Oil (CPO), and Distilled Pyrolysis Oil (DPO), as shown in Fig. 2, reveals differences in hydrocarbon distribution, widely influencing their suitability for catalytic cracking and olefin production. PPO exhibits the highest concentration of naphthene at 37% and iso-paraffins at 26%. It's important to note that while PPO shows promise for light olefin production, the presence of contaminants such as suspended carbon, sulfur, and dissolved solids in oils can pose challenges for their use as feedstocks in industrial crackers. These contaminants can lead to corrosion, increased coke formation, and catalyst deactivation. These features reduce PPO's overall effectiveness as a feedstock for maximizing light olefin yields. In contrast, DPO presents a more favourable composition for olefin production, with a lower naphthene content of 26% and a significant olefin fraction of 23%, the highest among the three oils. DPO also contains 23% paraffins, offering a good balance between reactivity and thermal stability, which supports efficient conversion with lower coke formation. The higher aromatics in DPO are offset by its superior olefin content, along with reduced naphthenes, allowing for a balanced feed that maximizes light olefin yields without excessive coke production. CPO is considered an intermediate feedstock between PPO and DPO. It has the highest paraffin content at 30%, with moderate olefin (16%) and naphthene (29%) levels. The iso-paraffin fraction in CPO is 19%, higher than in DPO but lower than in PPO, suggesting a structured hydrocarbon framework that offers moderate cracking reactivity. The relatively lower olefin content and presence of higher naphthenes make CPO slightly less optimal than DPO for the present reaction conditions. The detailed GC-MS composition of DPO is presented in the SI (Table S6).

Table 1 reports the physical properties of upgraded oil. The density of DPO is slightly above the typical range reported for aromatic naphtha (0.60 to 0.76 g cm^{-3}).[28] The viscosity of all three oils is significantly lower than that of typical naphtha (4.28 cSt at 40 °C).[29] The API gravity at 60 °F for all three oils exceeds 35° API, classifying them as light oils. All three oils show almost similar carbon content. The carbon content of PPO (84.63%), DPO (85%), and CPO (84.75%) is nearly identical. Notably, PPO contains 0.07% sulfur during large-scale manufacture, whereas ordinary naphtha contains less than 2 ppm sulfur.[30] In addition to PIONA analysis, the Motor Octane Number (MON) of DPO was found to be 55.7, higher than that of CPO (52.6). This difference suggests a higher degree of unsaturation in DPO. This inference is further supported by the Bromine number,

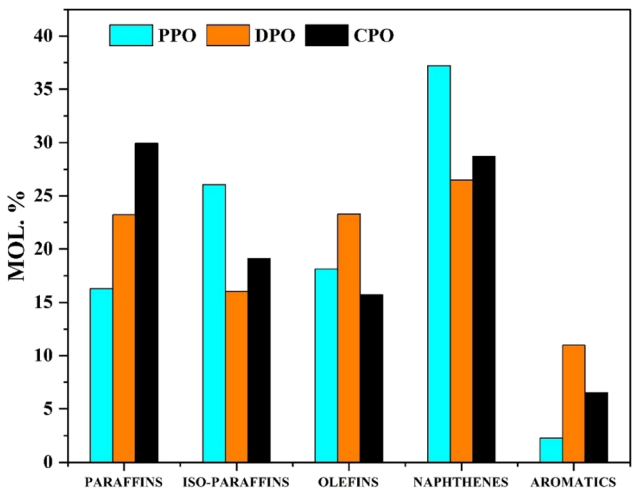

Fig. 2 PIONA analysis of oil.

Table 1 Properties of oils used in the study[a]

Properties	PPO	CPO	DPO
Avg. molecular weight	—	140.9	141.8
Calculated octane no.	—	55.6	59
Motor octane no. (Jenkins)	—	52.6	55.7
Bromine no.	—	4.7	7.8
Density (g cm^{-3})	0.789	0.774	0.767
Viscosity (cSt)	1.49	0.95	0.90
C (%)	84.63	84.75	85.0
H (%)	15.2	15.2	14.5
N (%)	0.10	0.01	0.50
S (%)	0.07	0.04	—
Cl (ppm)	2.13	0.89	0.09
Al (ppm)	0.013	<LOD	<LOD

[a] (*Without oxygen), LOD – limits of detection.

which also indicates a higher concentration of unsaturated in DPO compared to CPO. Chlorine content decreased in DPO than PPO due to combined chemical treatment and oxidation rather than distillation alone. Owing to the presence of metal impurities, PPO exhibited higher contaminant levels; however, after chemical upgradation, a significant reduction was observed in DPO, indicating the effective removal of metal contaminants during the upgrading process.[31]. Fig. S4 presents the true boiling point (TBP) curve of the upgraded oil, further illustrating its improved distillation characteristics.

3.2 Catalyst characterization

Fig. 3 shows the E-CAT characteristics for its suitability in the catalytic cracking experimentation. BET results are reported in

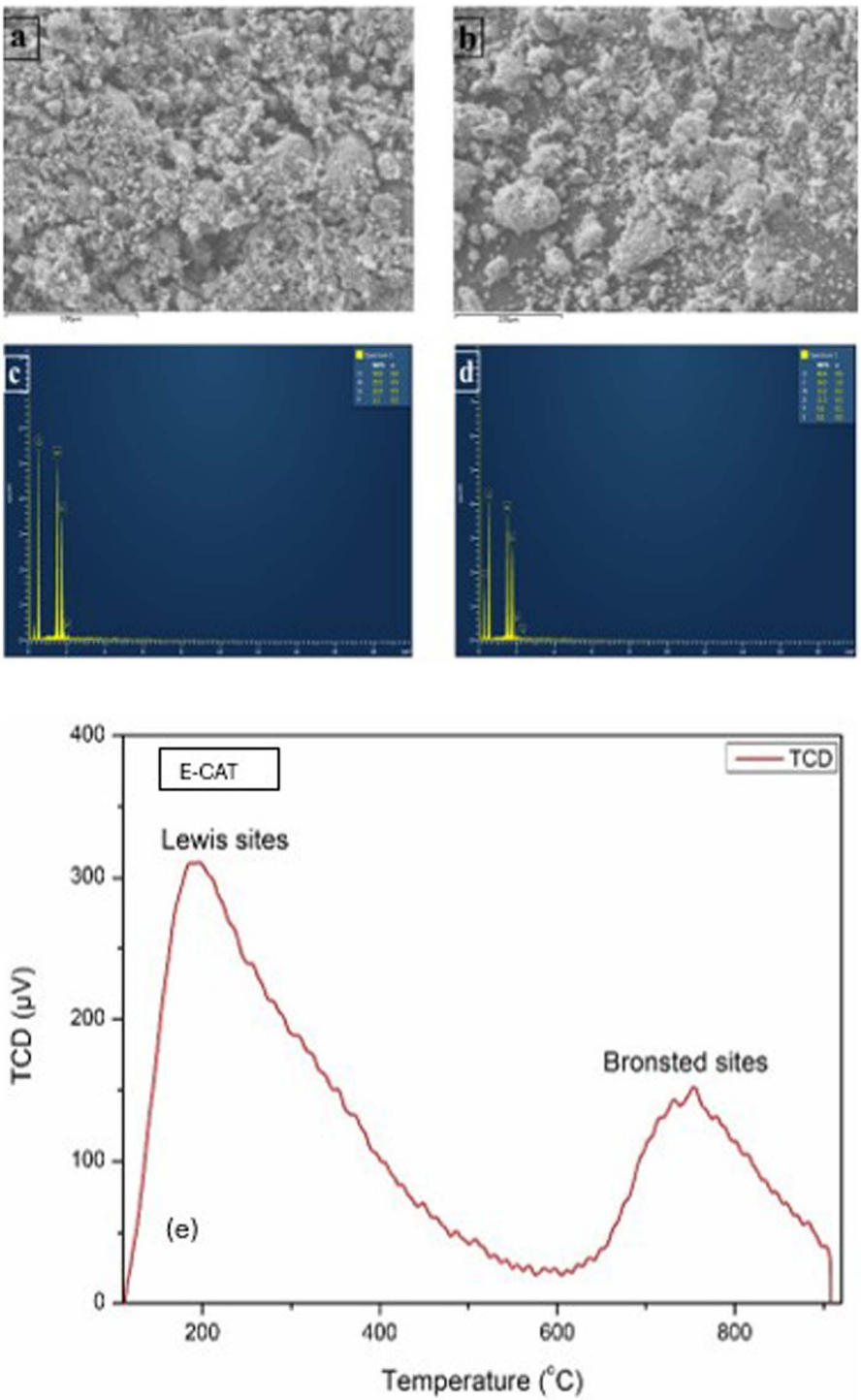

Fig. 3 (a) FESEM image of E-CAT (before experiment), (b) FESEM image of spent E-CAT (after experiment), (c) EDX analysis of E-CAT, (d) EDX analysis of spent E-CAT, (e) NH_3-TPD of E-CAT.

Table 2 BET and EDX analysis of regenerated and used catalysts

Sample	Surface area ($m^2\ g^{-1}$)	Total pore volume ($cm^3\ g^{-1}$)	Average pore diameter (nm)	Al (wt%)	Si (wt%)	O (wt%)	P (wt%)	C (wt%)
E-CAT	54.632	0.1165	11.897	25	22.9	50.9	1.2	—
Spent E-CAT	35.898	0.0827	13.304	13.2	11.5	40.4	0.6	34.3

Table 2. as the E-CAT has a surface area notably lower than that of the fresh FCC catalyst, which is around 120 to 270 $m^2\ g^{-1}$. Additionally, the total pore volume decreased from 0.1165 $cm^3\ g^{-1}$ to 0.082759 $cm^3\ g^{-1}$. However, the average pore diameter increased from 8.5264 nm to 9.2214 nm. Coke deposition within the catalyst's porous network is suggested by this inverse trend, which could partially block smaller pores and reduce the number of reaction-active sites available. The activity profile, based on NH_3-TPD, was analyzed in terms of Lewis and Brønsted sites and the total acidity. The NH_3-TPD profile shows two major desorption peaks after deconvolution, the peak around 184 °C corresponds to weak acid sites (0.144 mmol g^{-1}), while the peak at 754 °C corresponds to strong acid sites (0.085 mmol g^{-1}). The total acidity of the E-CAT is 0.277 mmol g^{-1}. This acid site trend[32] shows that ammonia gets adsorbed and needs a higher temperature to desorb from the Lewis sites.

The main issue is the accumulation of coke, which is known to impede mass transfer and diffusion within the catalyst, resulting in the loss of catalytic efficiency over time. The shift in elemental composition seen in the EDX results of the spent catalyst points to coke accumulation as a major contributor to its loss of activity. The degree of carbonaceous buildup during the reaction is demonstrated by the significant increase in carbon content, which went from an undetectable level in the regenerated catalyst to 34.3 wt% in the used catalyst. Simultaneously, the concentrations of aluminium (Al) and silicon (Si) declined from 25 wt% to 13.2 wt% and 22.9 wt% to 11.5 wt%, respectively. This depletion suggests that coke may leach or mask active sites, impairing catalyst performance. The degree of deactivation during the reaction was also confirmed by the FESEM imaging analysis of the spent catalyst, which showed notable structural changes to the catalyst after reactions. The catalyst's FESEM imaging after the experiment showed a very uneven and rough surface morphology, further supporting the accumulation of coke. Substantial pore blockage is indicated by the noticeable presence of particle agglomeration and thick carbonaceous deposits on the catalyst surface, which supports the results of the BET and EDX analyses.[33] An FTIR study *via* ATR mode was performed to clarify the functional group and difference of E-CAT and spent E-CAT, and the results are shown in Fig. S3.[34]

3.3 Parametric effect on olefin production

3.3.1 Effect of weight hourly space velocity. The WHSV crucially influences olefin production during catalytic cracking. As depicted in Fig. 4. and detailed in SI Table S1, varying WHSV alters the hydrocarbon product distribution. Low WHSV was not favorable for the product yield, likely due to the higher residence time between the catalyst and reactants. Higher WHSV was preferred for optimizing activity, which enabled a shorter contact time for the catalyst to activate the reactant's behaviour.[35–37] The methane content at higher WHSV (2 h^{-1}) also dropped to 17 mol% at 550 °C, as shorter residence times limited excessive cracking. At a low WHSV (0.5 h^{-1}), the olefin content was 26.4 mol%, remarkably lower than the 61.1 mol% achieved at a higher WHSV (2 h^{-1}). In Tran *et al.*'s study, the formation of C_2–C_3 olefins initially increased between 4 h^{-1} and

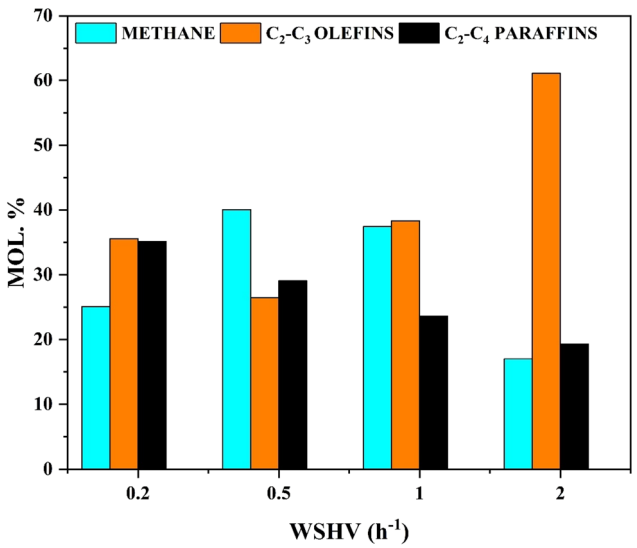

Fig. 4 Grouped products from cracking DPO under different WHSV (reaction conditions: 550 °C, WHSV = 0.2–2 h^{-1}).

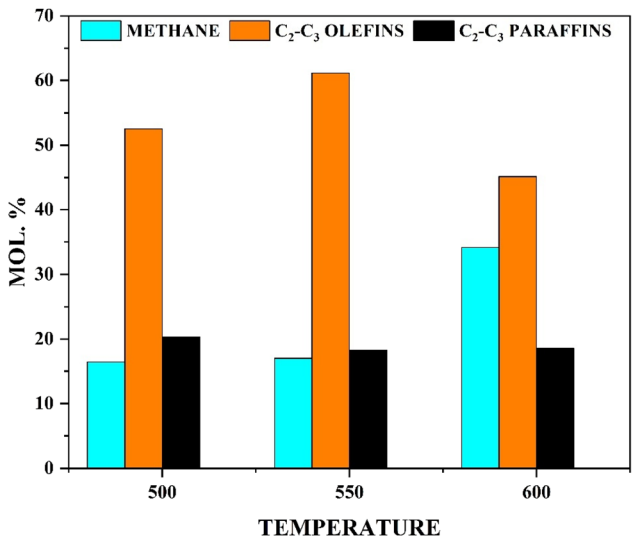

Fig. 5 Grouped products from cracking DPO at different temperatures (reaction conditions: 500–600 °C, WHSV = 2 h^{-1}).

8 h^{-1}, but then gradually declined as the WHSV rose from 16 h^{-1} to 48 h^{-1}. The selective formation of olefins is favoured by reduced hydrogen transfer reactions at higher WHSV, minimizing olefin hydrogenation into paraffins. In both studies, C_2–C_4 paraffin yields increased with a decrease in WHSV.

3.3.2 Effect of reaction temperature. The reaction temperature strongly influences the catalytic cracking of DPO over the E-CAT catalyst, and the results are shown in Fig. 5. at a fixed WHSV of 2 h^{-1}. High methane content was a measure of excessive cracking, increasing with temperature from 16.4 mol% at 500 °C to 17 mol% at 550 °C, and then doubling to 34.1 mol% at 600 °C. A similar trend of increasing methane was noted in Tran *et al.*'s study, where methane content increased gradually with temperature. C_2–C_3 olefin content peaked at a remarkable 61.1 mol% at 550 °C, rising from 52.5 mol% at 500 °C, and then decreasing to 45.1 mol% at 600 °C, whereas Tran *et al.*'s reported an increase in C_2–C_3 olefin content with temperature. In both studies, C_2–C_4 paraffin content remained relatively stable, showing minimal fluctuations with temperature. The current study showed that the ideal cracking temperature for DPO processing with the FCC catalyst was 550 °C. The yield of useful C_2–C_3 olefins was maximized at this temperature, while the production of less desirable products such as methane and C_2–C_4 paraffins was minimized. Inadequate olefin production resulted from inadequate energy input below 550 °C and excessive energy beyond 550 °C. The detailed compositional analysis of constituent gases is further mentioned in the SI (Table S2).

3.4 Comparative analysis of olefin production

3.4.1 Effect of oil type. The distribution of products during catalytic cracking was strongly influenced by the feedstock selection due to variations in PIONA content.[38] Fig. 6 shows grouped products from cracking PPO, DPO, and CPO under fixed reaction conditions: 550 °C, WHSV = 2 h^{-1} (detailed in SI Table S3). The DPO, with its purity and higher concentration of unsaturated hydrocarbons such as olefins, indicated increased reactivity and reduced catalyst deactivation[38] during cracking, leading to high production of olefins (61.1 mol%). In contrast, CPO, which underwent chemical treatment, contained fewer unsaturated hydrocarbons, resulting in lower reactivity and consequently lower C_2–C_3 olefin production (44.8 mol%). PPO resulted in lower C_2–C_3 olefin yields (43.3 mol%) due to impurities, such as sulfur. Methane production is highest in CPO (26.4%), closely followed by PPO (25.7 mol%), while DPO shows a significantly lower yield (17 mol%).

3.4.2 Effect of time stream on ethylene and propylene production. The production patterns of ethylene and propylene from CPO and DPO evolved quite differently over time, even though both were cracked under the same conditions (550 °C, WHSV = 2 h^{-1}) (refer Fig. 7 and further details in SI, Tables S4 and S5). During the early reaction period, the catalyst maintained an efficient pathway to produce ethylene and propylene consistently. Ethylene production from CPO showed a slight decline in the early stage, falling from 20.4 mol% to 16.88 mol% by the second hour. This was followed by a gradual rise, peaking at 23.5 mol% around the tenth hour, after which the values remained relatively steady between 18.46 mol% and 19.75 mol% for the rest of the reaction period. The catalyst maintained its selectivity after the first hour for propylene, resulting in a steady output ranging from 22.74 mol% to 28.53 mol%. The average methane production over time was notably lower in DPO in contrast to CPO. Initially, the elevated unsaturation levels enhanced olefin selectivity. However, the gradual accumulation of coke on the catalyst's active sites led to a reduction in its activity, which altered reaction pathways and thereby diminished its effectiveness.[39] DPO showed a notable fall in ethylene yield, from 31.09 mol% during the first hour to just 12.13 mol% by the fourth hour, suggesting that coke production quickly deactivated the sites responsible for ethylene generation. Despite this, propylene levels stayed high

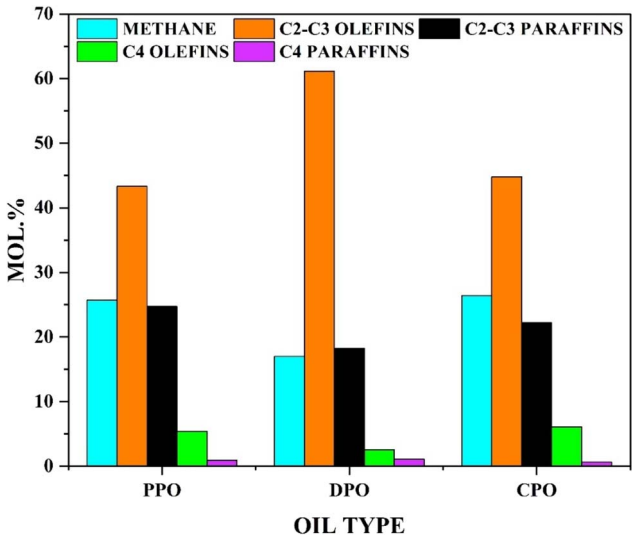

Fig. 6 Grouped products from cracking PPO, DPO, and CPO (reaction conditions: 550 °C, WHSV = 2 h^{-1}).

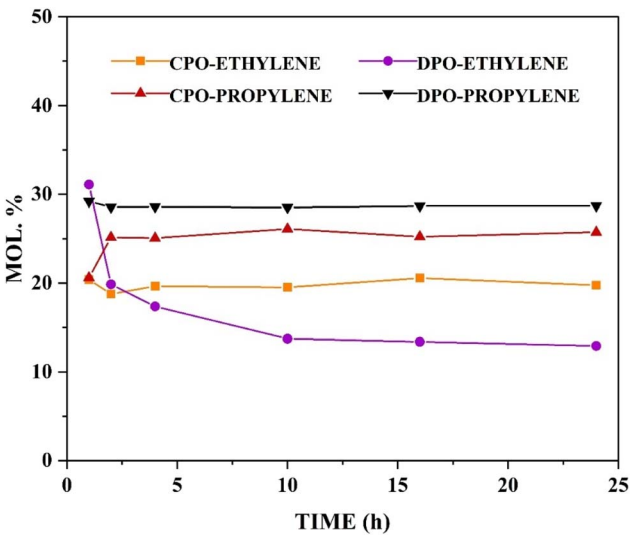

Fig. 7 Ethylene and propylene production over time at 550 °C and a WHSV of 2 h^{-1}.

Table 3 Comparison of catalytic cracking results for PPO, CPO, and DPO in a fixed bed system and WPPO in a fluidized bed setup

Properties	Catalytic cracking (present work)			Ref. 41
Feed	PPO	CPO	DPO	WPPO
Reactor type	Fixed-bed	Fixed-bed	Fixed-bed	Fluidized bed
Feed rate	2 h^{-1}	2 h^{-1}	2 h^{-1}	1000 g h^{-1}
Operating temperature	550 °C	550 °C	550 °C	659 °C
Feed composition (%)				
Aromatics (%)	2.26	8.07	10.97	17.0
Olefins (%)	17.42	15.73	23.29	27.3
Paraffin (%)	16.31	29.93	23.20	18.8
Iso-paraffin (%)	26.06	19.12	16.05	7.0
Naphthene (%)	37.21	28.70	26.49	6.5
Product yield	mol%	mol%	mol%	wt%
P/*E* ratio	1.01	0.89	0.93	2.1
Methane	25.70	26.40	17.0	3.6
Ethylene	20.4	22.9	31.09	10.3
Propylene	20.6	20.5	29.19	12.6

and constant throughout, continuously exceeding 27 mol%. In the case of PPO, it is effective in producing ethylene and propylene in the first hour; however, over a longer duration, it can lead to the accumulation of heavier hydrocarbon, and from an industrial point of view and to separate these fractions from the desired light olefins, extra steps and equipment are required, which makes the separation and purification process much more complex and expensive when heavy hydrocarbons are present. The sulfur content and impurities in PPO accelerate catalyst deactivation. Additionally, heavy hydrocarbons have a tendency to foul the reactor, which can result in operational problems and increased maintenance needs that negatively impact overall productivity, indicating a need for a cleaner feedstock.[40]

3.4.3 Comparative assessment of ethylene and propylene production. DPO performed best in the fixed bed reactor at 550 °C and a WHSV of 2 h^{-1}, producing 31.09 mol% ethylene and 29.19 mol% propylene, with a total C_2–C_3 olefin yield of 61.1 mol% (refer Table 3). The circulating fluidized bed reactor data reported by Tran *et al.* showed a different pattern. WPPO cracked at 659 °C and a feed rate of 1000 g h^{-1} produced 10.3 wt% ethylene and 21.4 wt% propylene, giving a *P*/*E* ratio of 2.1. The high temperature and short residence time inside the circulating fluidized bed reactor favoured ethylene formation. The circulating fluidized bed reactor produced 44.3 wt% of C_2–C_4 olefins. Overall, upgrading the feed from PPO to CPO and then DPO improved light-olefin production. The fixed-bed reactor produced a more balanced product in terms of *P*/*E* ratio mixture than the circulating fluidized bed reactor, which mainly yielded propylene.

4 Conclusion

This study examined the feasibility of using crude and upgraded waste plastic pyrolysis oils (PPO, CPO, and DPO) for light olefin production through catalytic cracking in a fixed bed reactor. Although the configuration differs from industrial steam crackers, the selected operating conditions were designed to emulate comparable thermal cracking environments, providing insight into feedstock upgradation and olefin selectivity. The results indicate that this objective was achieved, with upgraded oils showing improved cracking performance and light olefin selectivity compared with waste plastic pyrolysis oil. The observed trends reflect the relative suitability of upgraded plastic oils for light olefin production when compared with conventional steam cracking feedstocks. Among the tested feedstocks, DPO showed the highest performance, yielding 61.1 mol% C_2–C_3 olefins at 550 °C and 2 h^{-1} WHSV. The reaction-parameter study revealed that at a temperature of 550 °C, a low WHSV favoured methane formation, whereas a higher WHSV led to enhanced light olefin selectivity and reduced methane formation. The fixed bed reactor promoted a balanced *P*/*E* ratio, whereas the fluidized bed reactor favored propylene production over ethylene. Overall, upgrading waste plastic oils through chemical purification and distillation markedly improved their composition and cracking efficiency. While the reaction set-up differs from commercial crackers, the observed product trends and coke-suppression behaviour align with industrial mechanisms, pointing to the potential of upgraded pyrolysis oils as sustainable, circular feedstocks for olefin production and as a pathway to reduce dependence on fossil-based naphtha.

Author contributions

Abhishek G. Sarang: investigation, data curation, analysis, writing – original draft; Aditya Bora: analysis, writing – original draft; Syed Mohammed Razak: methodology, analysis, writing & editing; Karan Sharma: investigation, analysis; Chandan Kumar Munagala: investigation, resources, writing & editing; Pratik

Mali: analysis; Nettem V. Choudary: conceptualization; Vineet Aniya: conceptualization, funding acquisition, supervision.

Conflicts of interest

The authors declare that they have no known competing financial interests or personal relationships that could have appeared to influence the work reported in this paper.

Abbreviations

ASTM	American Society for Testing and Materials
ATR	Attenuated Total Reflectance
BET	Brunauer–Emmett–Teller
CAGR	Compound Annual Growth Rate
PPO	Plastic Pyrolysis Oil
CPO	Chemically Treated Plastic Oil
CFBR	Circulating Fluidized Bed Reactor
DPO	Distilled Plastic Oil
FCC	Fluidized Catalytic Cracking
E – Cat	Equilibrium Catalyst
EDX	Energy Dispersive X-ray
FESEM	Field Emission Scanning Electron Microscopy
FTIR	Fourier Transform Infrared Spectroscopy
FID	Flame Ionization Detector
GC	Gas Chromatography
CWS	Cold Water Supply
MS	Mass Spectrometer
PIONA	Paraffin, Iso-Paraffin, Olefin, Naphthenes, Aromatics
RBF	Round-Bottled Flask
NH_3-TPD	Ammonia Temperature Programmed Desorption
WHSV	Weight Hourly Space Velocity
WPPO	Waste Plastic Pyrolysis Oil

Data availability

Data will be provided upon reasonable request.

Supplementary information (SI) is available. See DOI: https://doi.org/10.1039/d5su00937e.

Acknowledgements

We thank the Director, CSIR-IICT (Ms. No. IICT/Pubs./2025/292), for providing all the required facilities to carry out the work. The authors sincerely acknowledge Mangalore Refinery and Petrochemicals Limited (MRPL) for generously providing the E-CAT catalyst used in this study.

References

1 R. Analysis, Propylene Market Size, Share, Trends & Insights Report, 2035, Accessed: Nov. 10, 2024, https://www.rootsanalysis.com/propylene-market.
2 EY, How petrochemical industry in India drives growth with investment and innovation, Accessed: Nov. 12, 2024, https://www.ey.com/en_in/insights/energy-resources/how-petrochemical-industry-in-india-drives-growth-with-investment-and-innovation.
3 P. Wattanapaphawong, *et al.*, Effect of carbon number on the production of propylene and ethylene by catalytic cracking of straight-chain alkanes over phosphorus-modified ZSM-5, *Fuel Process. Technol.*, 2020, **202**, 106367, DOI: 10.1016/j.fuproc.2020.106367.
4 Y. Xu, *et al.*, Targeted Catalytic Cracking to Olefins (TCO): Reaction Mechanism, Production Scheme, and Process Perspectives, *Engineering*, 2023, **30**, 100–109, DOI: 10.1016/j.eng.2023.02.018.
5 J. Chateau, G. Dang, M. MacDonald, J. Spray and S. Thube, *A Framework for Climate Change Mitigation in India*, IMF Working Paper (WP/23/218), 2023.
6 P. G. C. Nayanathara Thathsarani Pilapitiya, *et al.*, The world of plastic waste: A review, *Clean. Mater.*, 2024, **11**, 100220, DOI: 10.1016/j.clema.2024.100220.
7 M. Kan, *et al.*, Environmental impacts of plastic packaging of food products, *Resour. Conserv. Recycl.*, 2022, **180**, 106156, DOI: 10.1016/j.resconrec.2022.106156.
8 R. Kumar, *et al.*, Impacts of Plastic Pollution on Ecosystem Services, Sustainable Development Goals, and Need to Focus on Circular Economy and Policy Interventions, *Sustainability*, 2021, **13**(17), 9963, DOI: 10.3390/su13179963.
9 M. S. Qureshi, *et al.*, Pyrolysis of plastic waste: Opportunities and challenges, *J. Anal. Appl. Pyrolysis*, 2020, **152**, 104804, DOI: 10.1016/j.jaap.2020.104804.
10 M. J. B. Kabeyi, *et al.*, Review and Design Overview of Plastic Waste-to-Pyrolysis Oil Conversion with Implications on the Energy Transition, *J. Energy*, 2023, **2023**, 1–25, DOI: 10.1155/2023/1821129.
11 A. Eschenbacher, *et al.*, Highly selective conversion of mixed polyolefins to valuable base chemicals using phosphorus-modified and steam-treated mesoporous HZSM-5 zeolite with minimal carbon footprint, *Appl. Catal., B*, 2022, **309**, 121251, DOI: 10.1016/j.apcatb.2022.121251.
12 M. Kusenberg, *et al.*, A comprehensive experimental investigation of plastic waste pyrolysis oil quality and its dependence on the plastic waste composition, *Fuel Process. Technol.*, 2022, **227**, 107090, DOI: 10.1016/j.fuproc.2021.107090.
13 M. M. Hasan, *et al.*, Pyrolysis of plastic waste for sustainable energy recovery: Technological advancements and environmental impacts, *Energy Convers. Manage.*, 2025, **326**, 119511, DOI: 10.1016/j.enconman.2025.119511.
14 M. Kusenberg, *et al.*, Contaminant removal from plastic waste pyrolysis oil via depth filtration and the impact on chemical recycling: A simple solution with significant impact, *Chem. Eng. J.Oct*, 2023, **473**, 145259, DOI: 10.1016/j.cej.2023.145259.
15 A. Pumpuang, *et al.*, The influence of plastic pyrolysis oil on fuel lubricity and diesel engine performance, *RSC Adv.*, 2024, **14**(14), 10070–10087, DOI: 10.1039/D3RA08150H.
16 B. T. Ramesh, *et al.*, Extraction and Performance Analysis of Hydrocarbons from Waste Plastic Using the Pyrolysis Process, *Energies*, 2022, **15**(24), 9381, DOI: 10.3390/en15249381.

17 F. Faisal, *et al.*, Waste plastics pyrolytic oil is a source of diesel fuel: A recent review on diesel engine performance, emissions, and combustion characteristics, *Sci. Total Environ.*, 2023, **886**, 163756, DOI: 10.1016/j.scitotenv.2023.163756.
18 I. Oluwoye, *et al.*, Controlling NOx emission from boilers using waste polyethylene as reburning fuel, *Chem. Eng. J.*, 2021, **411**, 128427, DOI: 10.1016/j.cej.2021.128427.
19 M. I. Jahirul, *et al.*, Automobile fuels (diesel and petrol) from plastic pyrolysis oil—Production and characterisation, *Energy Rep.*, 2022, **8**, 730–735, DOI: 10.1016/j.egyr.2022.10.218.
20 H. Raghav, *et al.*, Catalytic pyrolysis of low-density waste polyethylene into light olefins and hydrogen over manganese-supported alumina, *J. Environ. Chem. Eng.*, 2025, **13**(1), 115254.
21 Y. Diao, *et al.*, Tandem catalytic cracking of LDPE to C_2–C_4 olefins over interconnected NZ@Al-meso-SiO_2: Role of hierarchical porosity and acidity, *Appl. Catal. A: Gen.*, 2025, **708**, 120538.
22 P. Peng, *et al.*, Diffusion and catalyst efficiency in hierarchical zeolite catalysts, *Natl. Sci. Rev.*, 2020, **7**(11), 1726–1742, DOI: 10.1093/nsr/nwaa184.
23 L. Zhang, *et al.*, Insight into the impact of Al distribution on the catalytic performance of 1-octene aromatization over ZSM-5 zeolite, *Catal. Sci. Technol.*, 2019, **9**(24), 7034–7044, DOI: 10.1039/C9CY01672D.
24 X. Xiao, *et al.*, Tuning the density of Brønsted acid sites on mesoporous ZSM-5 zeolite for enhancing light olefins selectivity in the catalytic cracking of n-octane, *Microporous Mesoporous Mater.*, 2022, **330**, 111621, DOI: 10.1016/j.micromeso.2021.111621.
25 S. Dong, *et al.*, Catalytic conversion of model compounds of plastic pyrolysis oil over ZSM-5, *Appl. Catal., B*, 2023, **324**, 122219, DOI: 10.1016/j.apcatb.2022.122219.
26 X. T. Tran and D. K. Kim, Maximizing light olefin production via one-pot catalytic cracking of crude waste plastic pyrolysis oil, *Fuel*, 2024, **361**, DOI: 10.1016/j.fuel.2023.130703.
27 B. Alawa, *et al.*, Discernment of synergism in co-pyrolysis of HDPE and PP waste plastics for production of pyro-oil: Mechanistic investigation with economic analysis and health risk assessment, *Process Saf. Environ. Prot.*, 2023, **169**, 107–131, DOI: 10.1016/j.psep.2022.10.077.
28 Bharat Petroleum, https://www.bharatpetroleum.in/our-businesses/industrial-and-commercial/industrial-fuel-products/fuels.aspx, Accessed: Nov. 12, 2024.
29 Cross Oil, https://crossoil.com/wp-content/uploads/2015/01/PDS-Heavy-Hydrotreated-Naphtha.pdf, Accessed: Nov. 12, 2024.
30 S. M. Razak, *et al.*, Hydrogen production potential from plastic pyrolysis oil: Experimental and economic insights, *J. Environ. Chem. Eng.*, 2024, **12**(2), 112220, DOI: 10.1016/j.jece.2024.112220.
31 L. Qi, Removal of Chlorine Ions from Desulfurization Wastewater by Modified Fly Ash Hydrotalcite, *ACS Omega*, 2020, **5**, DOI: 10.1021/acsomega.0c04074.
32 A. Ahmad, A. A. Al-Shammari, *et al.*, The Investigation of Zeolite to Matrix Ratio Effect on the Performance of FCC Catalysts during Catalytic Cracking of Hydrotreated VGO, *Catalysts*, 2023, **13**(9), 1255, DOI: 10.3390/catal13091255.
33 Á. A. Amaya, *et al.*, The behavior of the surface Si/(Si+Al) ratio in the FCC catalyst deactivation, *J. Electron. Spectrosc. Relat. Phenom.*, 2019, **239**, 146932, DOI: 10.1016/j.elspec.2019.146932.
34 G. J. Antos *et al.*, *Catalytic Naphtha Reforming, Revised and Expanded*, CRC Press, 2004, DOI: 10.1201/9780203913505.
35 A. P. Silva, *et al.*, Naphtha Characterization (PIONA, Density, Distillation Curve and Sulfur Content): An Origin Comparison, *Energies*, 2023, **16**(8), 3568, DOI: 10.3390/en16083568.
36 M. Ayoub, *et al.*, Effects of operating parameters for dry reforming of methane: A short review, *EPJ Web Conf.*, 2021, **287**, 04015, DOI: 10.1051/e3sconf/202128704015.
37 J. Xu, *et al.*, Biogas reforming for hydrogen production over a Ni–Co bimetallic catalyst: Effect of operating conditions, *Int. J. Hydrogen Energy*, 2010, **35**(23), 13013–13020, DOI: 10.1016/j.ijhydene.2010.04.075.
38 N. Rahemi, *et al.*, Syngas production from reforming of greenhouse gases CH4/CO2 over Ni–Cu/Al2O3 nanocatalyst: Impregnated vs. plasma-treated catalyst, *Energy Convers. Manag.*, 2014, **84**, 50–59, DOI: 10.1016/j.enconman.2014.04.016.
39 H. T. T. Trang, *et al.*, Mechanistic and kinetic insights of the formation of allene and propyne from the C3H3 reaction with water, *J. Mol. Model.*, 2024, **30**(7), 226, DOI: 10.1007/s00894-024-06033-9.
40 G. Bozzano, *et al.*, Fouling phenomena in pyrolysis and combustion processes, *Appl. Therm. Eng.*, 2002, **22**(8), 919–927, DOI: 10.1016/S1359-4311(02)00009-1.
41 X. T. Tran, *et al.*, Catalytic Cracking of Crude Waste Plastic Pyrolysis Oil for Enhanced Light Olefin Production in a Pilot-Scale Circulating Fluidized Bed Reactor, *ACS Sustain. Chem. Eng.*, 2024, **12**(33), 12493–12503, DOI: 10.1021/acssuschemeng.4c03763.